

# 1

# BIBLIOGRAPHY

## I. Molecular fluorescence<sup>3,8,9</sup>

Fluorescence spectrometry is one of the most used spectroscopic methods in analytical and scientific measurements; one of the reasons is the high sensitivity of the method. The photochemical reaction starts when a molecule absorbs an electromagnetic radiation of an appropriate wavelength. An excited state of the molecule is then created and will undergo different transformations. The wavelength range used for such excitation is between 200 nm and 750 nm (ultraviolet and visible) corresponding to energies between 600 and 160 kJ/mol. What follows describes the characteristics of the fluorescence emission of an excited molecule in solution.

### I.1. Light absorption

Light is a form of electromagnetic radiation. The human eye can sense the light in the interval 400-750 nm in the electromagnetic spectrum, called the visible region. Spectrophotometry covers the ultraviolet (200-400 nm), the visible (400-750 nm) and the infrared (700-15000 nm) regions, where the two formers have the largest application.

The wavelength is inversely related to its energy, according to Planck-Einstein equation (1):

$$E = h\nu = h\frac{c}{\lambda} \quad (1)$$

h: Planck constant ( $6.626 \times 10^{-34}$  J.s)

$\nu$ : frequency of radiation ( $s^{-1}$ )

c: the speed of light ( $2.9979 \times 10^8$  m.s<sup>-1</sup>)

$\lambda$ : wavelength of the radiation (m).

Thus, UV radiation has greater energy than the visible light but shorter wavelength.

A molecule absorbs electromagnetic radiation and transforms from a ground state to an excited state, the energy difference between these two states is the energy of the absorbed photon. In ultraviolet and visible, the absorption results in an electronic transition in the atom or molecule. In the case of molecules, the electron's transition occurs from the highest occupied molecular orbital (HOMO) to the lowest unoccupied molecular orbital (LUMO). Compounds absorb light in different wavelengths according to their molecular structure. A molecule absorbs energy from light *via* an electron jump. An electron from an orbital of the molecule in the ground state is excited to an unoccupied orbital with higher energy level. The molecule then goes from a fundamental state to an excited state. The possible electronic transitions are:  $n \rightarrow \pi^*$ ,  $\pi \rightarrow \pi^*$ ,  $n \rightarrow \sigma^*$ ,  $\sigma \rightarrow \sigma^*$ .

*The Beer-Lambert law*

The transmittance  $T$  of a molecule is the measure of the fraction of light that passes through the sample at a given wavelength; it is expressed by equation (2).

$$T = \frac{I}{I_0} \quad (2)$$

where:

$I_0$ : Intensity of incident light;

$I$ : Intensity of the light after it has passed through the sample;

The absorbance  $A$  is the estimation of light absorbed by the sample and it is represented as:

$$A = -\log T = -\log \frac{I}{I_0} \quad (3)$$

The Beer-Lambert law expresses the variation of intensity of radiation  $I$  in a homogeneous medium, the absorbance is expressed as follows:

$$A = \varepsilon \times l \times c \quad (4)$$

$A$ : the absorbance of the solution;

$\varepsilon$ : molar absorption coefficient ( $\text{L} \cdot \text{mol}^{-1} \cdot \text{cm}^{-1}$ );

$l$ : the distance the light travels through the solution (cm);

$c$ : the concentration of the sample (mol/L).

The Beer-Lambert law allows the quantitative determination of the absorbing chromophores. Exceptions to this law include high concentrations of the solute and when there are solid impurities.

*Bathochromic shift and others*

The absorbance spectrum is the plot of absorbance *versus* the wavelength of the incident light. Shifts in absorption spectra, of a certain chromophore, happen due to the effect of substitution or a change in the environment. A shift to longer wavelengths is called a bathochromic shift (or a red shift). A shift to shorter wavelengths is called a hypsochromic shift (or a blue shift). An increase in the molar absorption coefficient is called the hyperchromic effect, the opposite is the hypochromic effect (Fig. 1).

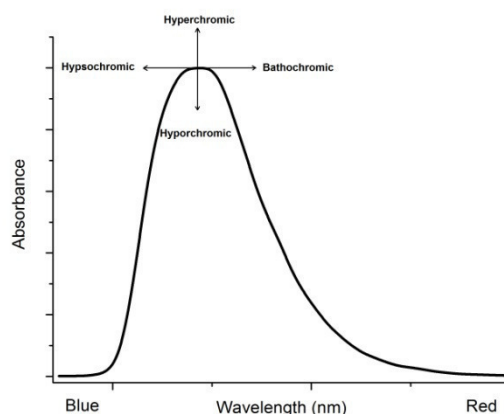


**Fig. 1.** Shifts in the absorption spectra.

### *Isosbestic points*

An isosbestic point is a wavelength where the absorbance values of two physical forms are equal and have the same absorption coefficient, representing a coordinate  $(\lambda, \epsilon)$ . The presence of an isosbestic point indicates that the stoichiometry of the reaction remains the same during the chemical reaction or the physical change of the sample.<sup>9</sup>

### **I.2. Fluorescence principles**

When a molecule absorbs light, three types of transitions occur: electronic, vibrational and rotational. In between electronic levels there are rotation and vibration levels. In order to create an electronically excited state, the molecule absorbs energy that is at least equal to the difference in energy between the highest occupied orbit (HOMO) and the lowest vacant orbital (LUMO) of the ground state. Electronic emission can be presented in two types: fluorescence and phosphorescence. Figure 2 displays the Perrin-Jablonski diagram where the possible photophysical processes in a molecular system: absorption, internal conversion (IC), fluorescence, intersystem crossing (ISC) and phosphorescence are described in a simple way. Absorption is very fast compared to the other processes. In the ground state of molecules, the molecular energies are constant and possess minimal values. When the molecule is irradiated, it absorbs the irradiation and an electronic transition takes place to higher electronic states. Electronic transitions occur when the molecule is irradiated by a specific wavelength. After a short time interval, the electrons return to the ground singlet state and energy is released in different radiative and non radiative fashions. When an electron gets excited, it rotates or vibrates down to the closest electronic level, the process is called internal conversion (IC), and it is a loss of energy in a non radiative fashion. When the electron goes down to the ground level, energy is emitted as a photon within the emission spectrum of the fluorophore.

This emission of a photon is called fluorescence, and it is a radiative relaxation. The photon emitted has longer wavelengths than the absorption wavelengths, hence a lower energy. Another process is the intersystem crossing (ISC). It is a non-radiative transition between two levels of different multiplicities (from a singlet to a triplet state of the molecule). Phosphorescence happens when an electron in the excited triplet state, due to ISC process, returns to the first electronic singlet state. Phosphorescence has a longer life time than fluorescence. Reverse intersystem crossing can occur, resulting in emission in the same spectral range as fluorescence called delayed fluorescence. Like fluorescence, phosphorescence and delayed fluorescence are both radiative relaxations.

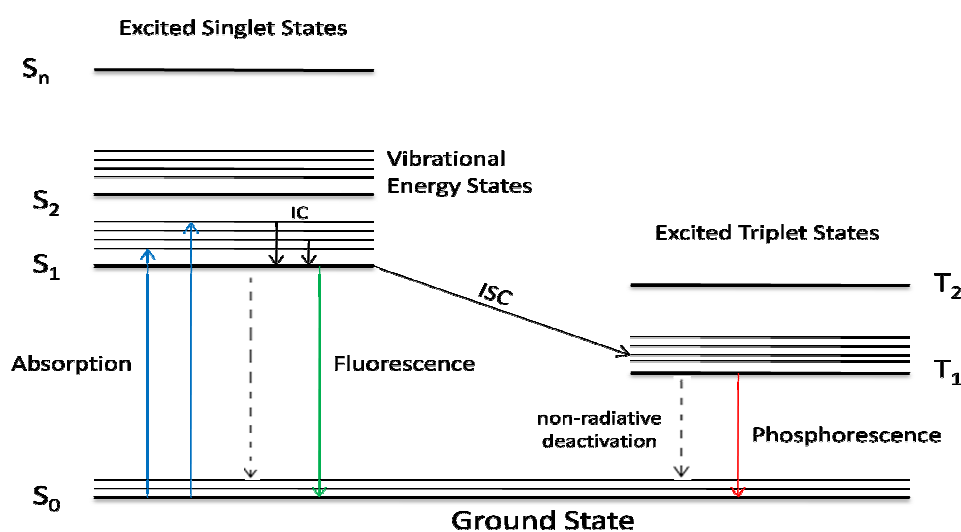


Fig. 2. The Perrin-Jablonski diagram.

### *Fluorescence quantum yield*

The fluorescence quantum yield is defined as the number of photons emitted per the total number of photons absorbed, with a maximum value of 1. It is usually determined by comparison with a fluorescence standard, where the standard and the sample should cover a similar  $\lambda$  range.<sup>9</sup>

### *Stokes Shift*

The Stokes shift is the difference, in nanometers or in frequency units, between the wavelength maximum of the absorption and the wavelength emission maximum. Each fluorophore has a distinct and individual Stokes Shift that can differ by changing the solvent. From a practical point of view, the detection of a fluorescent species is easier when the Stokes shift is larger.<sup>9</sup>

## Fluorescence quenching

Quenching is a deactivation of an excited molecular entity by an external environmental influence referred to as dynamic quenching, or by a substituent through a non-radiative process called static quenching.<sup>9</sup>

## II. Fluorescence detection strategies (Fluorescent chemosensor design)<sup>10-12</sup>

The fluorescence emission is strongly influenced by the surrounding medium, thus fluorescent molecules are used as probes for sensing different analytes in environmental and biological systems. A fluorescent chemosensor usually involves two components: a fluorophore and a guest receptor in a spaced or an integrated scaffold (Scheme 1). Once an analyte (guest) is bounded to the receptor, the photophysical characteristics of the sensor change *via* different mechanisms including photoinduced electron transfer (PET), intramolecular charge transfer (ICT) and others.



**Scheme 1.** (a) A spaced model for fluorescence sensing (b) An integrated model.

### II.1. Photoinduced Electron Transfer (PET)

One of the most commonly used strategies for developing fluorescent sensors is based on photoinduced electron transfer or PET sensing. A PET-type chemosensor model is composed of three units: fluorophore, spacer, and receptor as shown in Scheme 1 (a). Photoinduced electron transfer (PET) is often responsible for fluorescence quenching. As depicted in Fig. 3, upon excitation of the fluorophore an electron in HOMO goes to LUMO, if there is an orbital in the receptor part with energy level between HOMO and LUMO of the fluorophore, an electron transfer from HOMO of the receptor to the ground state orbital of the fluorophore takes place. The usual relaxation pathway is blocked and the emission is quenched. This is also called reductive photoinduced electron transfer. After the complexation with the analyte, the HOMO energy level of the receptor is reduced, not allowing the electron transfer, and this causes a fluorescence enhancement. As a consequence, weakly fluorescent chemosensors become strongly fluorescent when bonded with the analyte.

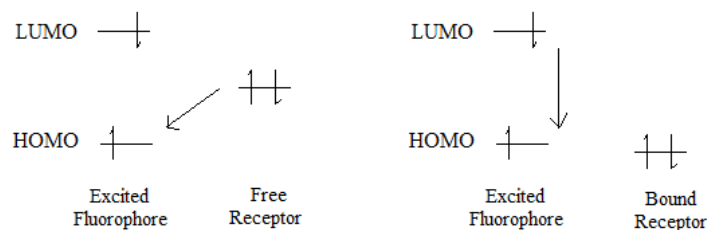


Fig. 3. Reductive PET mechanism.

In another case, the non-bonded sensor is fluorescent (oxidative PET mechanism), but once it is bonded to the analyte, the fluorophore acts as an electron donor, as illustrated in Fig. 4, and the fluorescence is quenched.

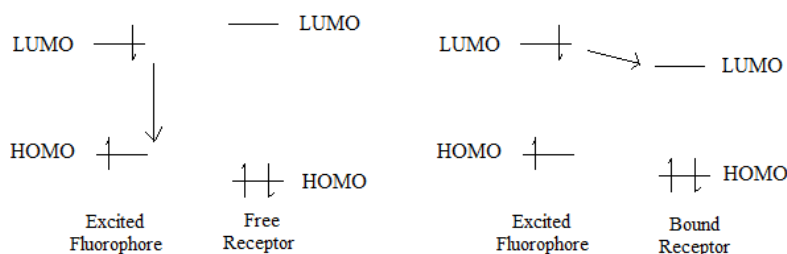


Fig. 4. Oxidative PET mechanism.

## II.2. Intramolecular Charge Transfer (ICT)

Intramolecular charge transfer is another mechanism that generally leads to a red or a blue shift in the absorption and/or emission spectra of a fluorophore. It is based on the integrated model (fluorophore–receptor) shown in Scheme 1 (b). Since there is no spacer in this kind of sensors, the receptor unit is part of  $\pi$ -electron system of the fluorophore, and an electron donating group (such as  $-\text{NH}_2$ ,  $-\text{NMe}_2$ ,  $-\text{CH}_3\text{O}$ ) of one part of the model is conjugated with an electron withdrawing group (like  $>\text{C}=\text{O}$ ,  $-\text{CN}$ ) of the other part of the sensor. Upon excitation of the molecule, an electron is promoted from one orbital to another leading to a change in the dipole moment of the fluorophore. When an analyte is reacted with either the donor or the acceptor part of the sensor, the ICT is perturbed, thus significant changes in the absorption and emission spectra are often observed.

## II.3. Energy Transfer (ET)

Energy transfer happens in multichromophoric dye systems. It is an energy transfer from an excited fluorophore (donor) absorbing at short wavelengths, to another fluorophore (acceptor) absorbing at longer wavelengths, and the emission of the donor partially overlaps with the absorption of the acceptor. There are two types of mechanisms for energy transfer: Förster type and Dexter type (Fig. 5). In the Förster type ET, the excited state donor (D)

transfers energy to the ground state acceptor (A). Dexter type ET is based on an electron exchange between the donor and the acceptor, and it usually happens in systems where donor and acceptor units are connected by a conjugated linker.

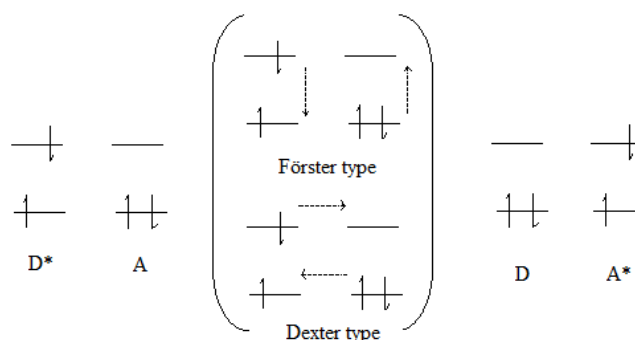
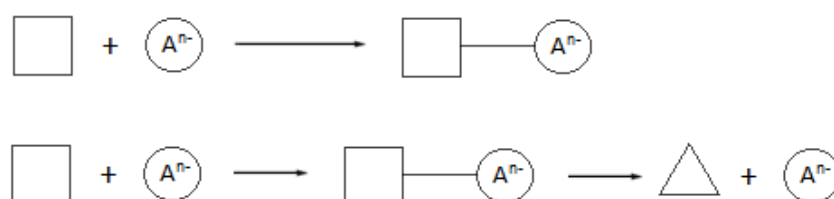


**Fig. 5.** Förster type and Dexter type mechanisms of energy transfer.

## II.4. Chemodosimeters

It is a new approach for the detection of analytes. Chemodosimeters show great selectivity and sensitivity. The term was first used for a fluorescent sensor for  $\text{Hg}^{2+}$  by a chemical reaction. When the analyte is an anion, it covalently bonds with the chemodosimeter, or it catalyzes a chemical reaction leading to the formation of a product with different optical properties (Scheme 2).



**Scheme 2.** Formation of chemodosimeter: anion adduct (top) and chemical reaction catalyzed by an anion (bottom).

Chemodosimeters display some disadvantages like long response time and irreversibility.

## II.5. Excimer formation

Excimers are dimmers formed by collision of a fluorophore in the excited state with the same fluorophore in the ground state. Excimers are often formed with fluorophores containing an extended conjugated  $\pi$ -system, like naphthalene, pyrene and acridine. The presence of an analyte can cause the assembly or association of an excimer, causing an enhancement or a quenching of the fluorescent band of the latter.

## III. Schiff bases as cyanide Chemosensors

A large number of sensors for cyanide anion has been designed in the recent years. Colorimetric and/or fluorimetric probes have attracted considerable interest for their simple



and fast implementation as well as their high sensitivity and selectivity. A lot of systems have been used for the detection of  $\text{CN}^-$  ion in organic and aqueous solutions, including, coumarin,<sup>5c,5d,6a,13-20</sup> BODIPY,<sup>21,22</sup> pyrene,<sup>23,24</sup> indole,<sup>25</sup> urea and thiourea based compounds,<sup>26,27</sup> phenazine,<sup>28</sup> boronic acid derivatives<sup>29</sup> and so on... Those systems detect cyanide anion throughout different mechanisms.

Among others, Schiff bases play an important role in the sensing field. They are generally easily prepared and show good selectivity to anions like fluoride and cyanide. Besides their anion-sensing abilities, Schiff bases were found to be selective to metals.<sup>30-34</sup> Herein we focus only on Schiff bases as cyanide chemosensors reported in the recent years.

Wu's group proposed two fluorescent chemosensors for the detection of cyanide in aqueous solution.<sup>29,35</sup> Compound **1** (Fig. 6) is a simple boronic acid derivative. The receptor showed a selective response to  $\text{CN}^-$  over other anions in  $\text{CH}_3\text{CN}/\text{H}_2\text{O}$  (2:8, v/v), presented by a color change from yellow to colorless, and a quenching in the fluorescence intensity. Job's plot and ESI-mass spectrometry indicated a 1:1 stoichiometry interpreted as a nucleophilic addition of  $\text{CN}^-$  to the imine moiety with an association constant of  $2.5 \times 10^4 \text{ M}^{-1}$  and a detection limit of 645 ppm. The mechanism was further confirmed by IR and  $^1\text{H}$  NMR spectroscopies. The sensor showed also selectivity to  $\text{CN}^-$  in D.I., lake ground, tap and drinking water.

The other compound is an oxime of 2-hydroxy-1-naphthaldehyde **2** (Fig. 6). When  $\text{CN}^-$  anion is added to a solution of the compound in  $\text{MeOH}/\text{H}_2\text{O}$  (1:9, v/v), a red shift in the absorbance and an enhancement in the fluorescence intensity were observed. The sensor was insensitive when treated with other anions. The complexation behavior of the receptor with  $\text{CN}^-$  was studied by  $^1\text{H}$  NMR titration experiments. The results showed a formation of hydrogen bonding between  $-\text{OH}$  group of the receptor and  $\text{CN}^-$ , with a 2:1 stoichiometry proposed by Job's plot and ESI-mass spectrometry analysis. The association constant for **2**- $\text{CN}^-$  was  $6.9 \times 10^{10} \text{ M}^{-2}$  and the detection limit was 17.9 ppm. The applicability of the sensor was tested in lake water and using indicator paper.

The naphthol derivative **3** (Fig. 6) was prepared and tested for its sensing properties.<sup>36</sup> It was found that the sensor is selective to  $\text{CN}^-$  anions in  $\text{DMSO}/\text{H}_2\text{O}$  (7:3, v/v) medium with a detection limit of 1.2  $\mu\text{M}$ . The fluorescence is turned on due to binding of  $\text{CN}^-$  followed by deprotonation of naphthalene  $-\text{OH}$  group, supported by  $^1\text{H}$  NMR titration. The sensor also exhibited a color change from colorless to yellow upon addition of  $\text{CN}^-$ . A 1:2 stoichiometry

was determined by Job's plot and ESI-mass spectrometry analysis. Paper strips were prepared and the compound was tested as live cell imaging reagent for intra-cellular detection of CN<sup>-</sup> anion in A549 cells.

Wei's group designed a new Schiff base **4** (Fig. 6) for the selective colorimetric and fluorometric detection of CN<sup>-</sup> anion in aqueous medium.<sup>6c</sup> The addition of CN<sup>-</sup> induced a charge transfer (ICT), causing changes in the absorption and emission properties of the probe. The detection limit was  $4.0 \times 10^{-7}$  M. The mechanism of the interaction was investigated by <sup>1</sup>H NMR spectroscopy, FTIR spectra and mass analysis and was proven to be a nucleophilic addition and a di-deprotonation of the –OH groups with a 1:2 stoichiometry.

The same group synthesized a Schiff base **5** (Fig. 6), from 2-hydroxy-1-naphthaldehyde and 2-aminopyridine.<sup>37</sup> The compound has good optical properties with a “naked-eye” colorimetric and fluorometric recognition of CN<sup>-</sup> in DMSO/H<sub>2</sub>O (9:1, v/v) solution and under acidic conditions. The solution turned from yellow to colorless with a blue fluorescence after addition of 50 equivalents of CN<sup>-</sup>, while the other studied anions did not cause any changes. The detection limit of the compound for CN<sup>-</sup> using UV-vis spectroscopy was  $3.9 \times 10^{-8}$  M, and using fluorescence spectroscopy was  $3.1 \times 10^{-9}$  M. Test strips were prepared to evaluate the practical applicability of the sensor. The binding mechanism was proved to be a nucleophilic addition by means of <sup>1</sup>H NMR titration and FTIR spectroscopy, and confirmed by DFT calculations.

Compounds **6a-6d** (Fig. 6), bearing a hydrazone moiety were also prepared by the same group and were tested for their sensing abilities in aqueous media.<sup>38</sup> The sensing ability of sensor **6a** was studied with different anions in DMSO/H<sub>2</sub>O (85/15, v/v, pH 7.20) binary solution using UV-vis spectroscopy. Only CN<sup>-</sup> gave a positive response, with detection limits of  $8 \times 10^{-5}$  and  $5 \times 10^{-6}$  M according to the visual color changes and UV-vis color changes, respectively. The same experiment was applied to the other compounds; **6b** was selective to CN<sup>-</sup> in DMSO/H<sub>2</sub>O (9:1, v/v) solution, while **6c** and **6d** showed no selectivity for the recognition of CN<sup>-</sup>. It is noticeable that only the compounds with a nitro group in the *para* position of the phenyl ring can selectively detect CN<sup>-</sup> ions. A possible mechanism, studied by <sup>1</sup>H NMR titration, includes a deprotonation of the –NH group. The alternative reversibility of probe **6a** was studied by addition of TFA. **6a** was also found to be a convenient colorimetric sensor for CN<sup>-</sup> by test strips.

Hu's group synthesized a selective fluorometric chemosensor **7** (Fig. 6) for the detection of  $\text{CN}^-$  anion in aqueous solution.<sup>39</sup> The compound comprises 2-hydroxy-1-naphthaldehyde and isoniazide functionalities. The probe showed fluorescence and UV-vis selectivity for  $\text{CN}^-$  in DMSO/ $\text{H}_2\text{O}$  (6:4, v/v) over other anions, with a detection limit of  $1.22 \times 10^{-9}$  M. The fluorescence enhancement is caused by an ICT process. The signaling mechanism was based on the deprotonation of hydroxyl and amino groups, supported by  $^1\text{H}$  NMR titration, IR and ESI-mass spectrometry analysis. Test strips were prepared to put into practice the use of the chemosensor.

The detection of  $\text{CN}^-$  and  $\text{F}^-$  using a pyrazine-derived chemosensor **8** (Fig. 6) was studied by Lee et al.<sup>40</sup> The sensor was easily prepared in a one step condensation between aminopyrazine and 2-hydroxy-1-naphthaldehyde. Cyanide was detected through a nucleophilic mechanism, while fluoride was detected through a deprotonation mechanism, with a 1:1 binding mode for both analytes, proposed by Job's plot,  $^1\text{H}$  NMR titration and ESI-mass spectrometry analysis. Only  $\text{F}^-$  and  $\text{CN}^-$  showed color changes in a 10% buffered solution through an ICT process. A color change from yellow to colorless was observed upon addition of  $\text{CN}^-$ , and from yellow to orange with  $\text{F}^-$ . DFT and TD-DFT calculations confirmed the sensing mechanisms of the two anions.

The same group developed a simple receptor **9** (Fig. 6) for the "naked-eye" detection of  $\text{CN}^-$  and  $\text{F}^-$  ions.<sup>41</sup> The sensor showed a selectivity to  $\text{CN}^-$  in DMSO/bis-tris buffer (1:5, v/v) solution interpreted by a color change from yellow to colorless due to a nucleophilic addition. For  $\text{F}^-$  anion, a color change from pale yellow to orange was detected in acetonitrile *via* a deprotonation mechanism. The blue shift of absorption after addition of  $\text{CN}^-$  in aqueous solution indicates a decrease in the ICT efficiency, and the detection limit was 105  $\mu\text{M}$  with an association constant ( $K$ ) of  $4.1 \times 10^2 \text{ M}^{-1}$ . The compound was found to detect  $\text{CN}^-$  anion over a pH range of 5-10. In the case of  $\text{F}^-$ , a red shift in the UV-vis spectra was rather observed, this might be explained by an increase in the electron density because of the deprotonation of  $-\text{OH}$  group. The association constant and the detection limit were  $1.7 \times 10^3 \text{ M}^{-1}$  and 60  $\mu\text{M}$ , respectively. The sensor showed good selectivity for fluoride with no interference of other anions except for  $\text{H}_2\text{PO}_4^-$ . The 1:1 stoichiometry of both analytes was obtained by Job's plot, ESI-mass spectrometry analysis and  $^1\text{H}$  NMR titration, and the interaction mechanisms were investigated by the latter.

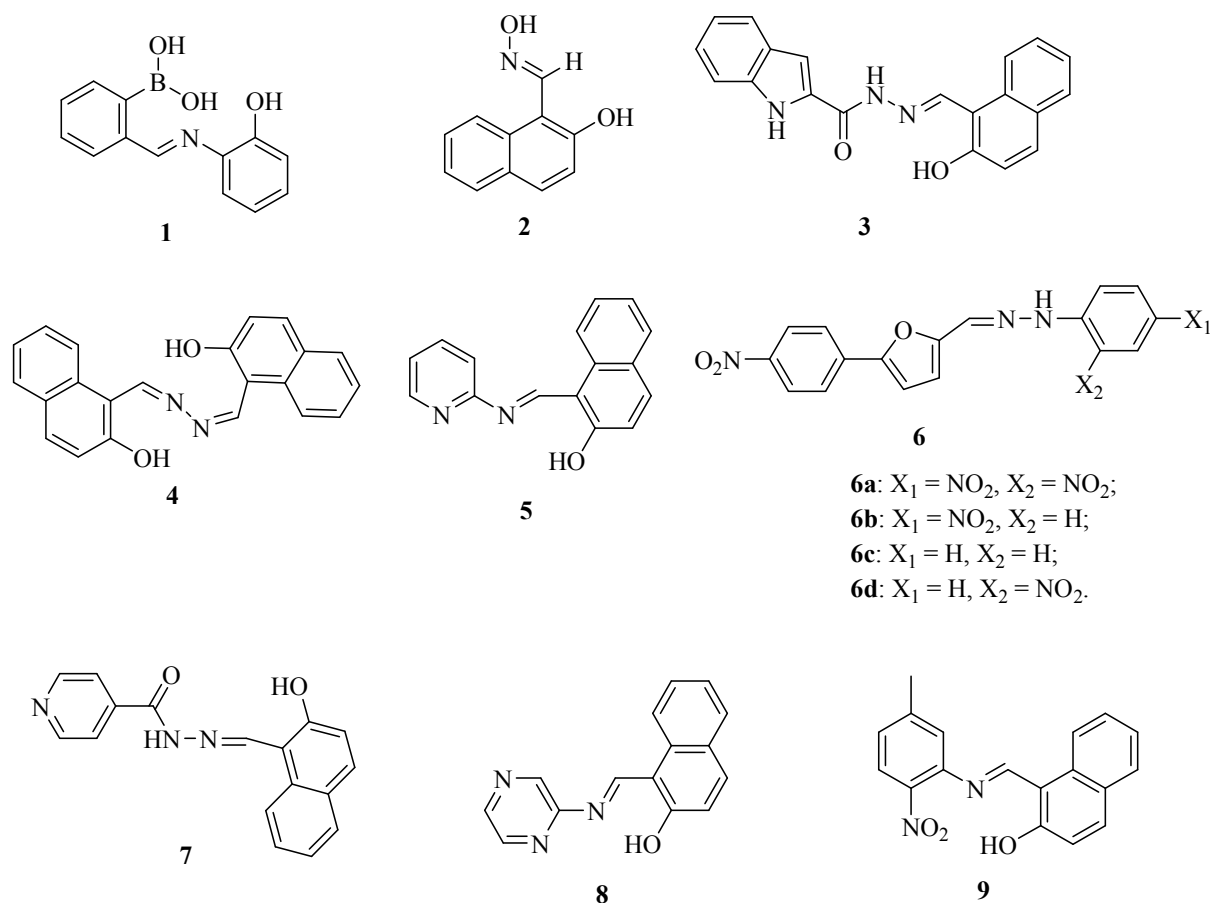


Fig. 6. Structures of chemosensors 1-9.

Another chemosensor for the detection of  $\text{F}^-$  and  $\text{CN}^-$  ions was developed.<sup>42</sup> The sensor is an azo linked Schiff base **10** (Fig. 7). Its sensing behavior was observed by “naked-eye” and confirmed by UV-vis spectroscopy, in the presence of different anions. The solution of the sensor in  $\text{CH}_3\text{CN}$  showed distinct color changes with  $\text{F}^-$ ,  $\text{AcO}^-$  and  $\text{CN}^-$ . In 20:80 water acetonitrile mixture,  $\text{CN}^-$  showed selective interaction with the sensor over other anions. The color changes to green and a red shift was observed in UV-vis spectrum. When the water is increased to 90%, the same results were obtained. The mechanisms of the interactions, supported by  $^1\text{H}$  NMR titration experiments, suppose that  $\text{F}^-$  anion interacts *via* hydrogen bonding with  $-\text{OH}$  group with a possibility of deprotonation, and  $\text{CN}^-$  *via* a nucleophilic addition to  $-\text{C}=\text{N}$  double bond. DFT calculations were used to better understand the behavior of receptor **10** with  $\text{F}^-$  and  $\text{CN}^-$  anions.

Zhang et al. designed a simple naphthalene chemosensor **11** (Fig. 7) for the detection of  $\text{F}^-$ ,  $\text{CN}^-$  and nitroaromatic explosives.<sup>43</sup> The sensor has a colorimetric selective detection of  $\text{F}^-$  and  $\text{CN}^-$  anions in a DMF/buffer (50:50, v/v) solution, with no changes upon addition of other anions. The interaction was found to be in 1:2 ratio for both anions.  $^1\text{H}$  NMR titrations

showed that  $F^-$  interacts *via* binding-deprotonation mechanism, while  $CN^-$  reacts *via* addition-deprotonation. The sensor was also sensitive to TNT and TNP by a “naked eye” experiment along with a quenching in the fluorescence intensity.

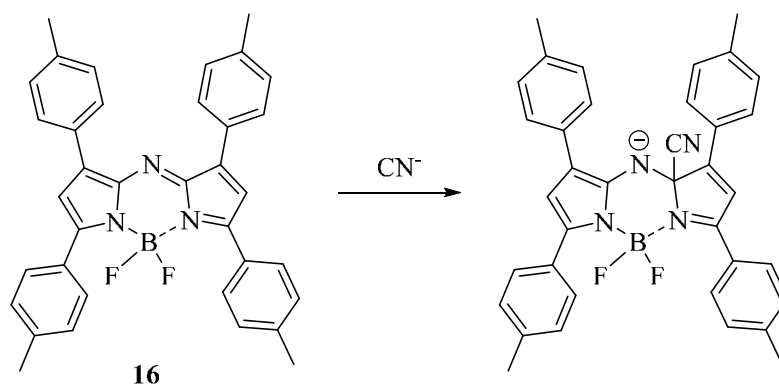
A colorimetric and turn-on fluorescence pyrene Schiff base receptor **12** (Fig. 7) for  $CN^-$  and  $F^-$  in acetonitrile solution was prepared.<sup>23</sup> The two anions displayed distinct color changes, while the other tested anions did not show any changes. The detection limits of the compound towards  $F^-$  and  $CN^-$  ions were determined to be 0.28 ppm and 0.41 ppm, respectively.  $^1H$  NMR titration and ESI-mass spectrometry experiments showed that  $F^-$  anion interacts by hydrogen bonding, while  $CN^-$  ion formed a new adduct by addition to the  $-C=N$  double bond.

Another new pyrene imine derivative **13** (Fig. 7) for fluorescent and colorimetric sensing of  $CN^-$ , this time in aqueous solution, and its application in bioimaging was reported.<sup>24</sup> The sensor was first tested in organic solution. The fluorescence and color changes were observed with  $CN^-$ ,  $AcO^-$ ,  $F^-$  and  $H_2PO_4^-$ , attributed to an ICT process. The detection limit was found to be  $1.48 \times 10^{-8}$  M for  $CN^-$ . When 10% of water was introduced into the system, the chemosensor displayed a selectivity towards  $CN^-$  interpreted by a color change of the solution and a fluorescence enhancement with a detection limit of  $1.08 \times 10^{-8}$  M. The chemosensor was employed in sensing  $CN^-$  within living HeLa cells.

The sensing abilities of compound **14** (Fig. 7) was evaluated in DMSO with eleven different anions.<sup>6d</sup> Addition of 1 equivalent of  $F^-$ ,  $CN^-$ ,  $AcO^-$ ,  $H_2PO_4^-$  and  $OH^-$  resulted in the development of two new bands in the UV-vis spectrum attributed to an ICT process resulting from hydrogen bonds between the compound and the anions. The red shift in the absorbance and the color changes were explained by a deprotonation of the  $-OH$  group. Crystal structure determination and DFT calculations were also carried out, as well as DNA-binding experiments.

The same authors reported another molecule of the same series **15** (Fig. 7),<sup>44</sup> where the Schiff base is prepared from salicylaldehyde instead of 2-hydroxy-1-naphthaldehyde. The compound was tested for its anion-sensing properties and DNA-binding ability. The sensor was found to be sensitive towards  $F^-$ ,  $OH^-$ ,  $AcO^-$  and  $CN^-$  in DMSO with selectivity for the detection of  $CN^-$  anion using fluorescence spectroscopy.

An aza-BODIPY **16** was reported as a colorimetric and turn-on fluorescence sensor for  $\text{CN}^-$  anion.<sup>22</sup> The compound is 1,3,5,7-tetraaryl aza-BODIPY, and can detect  $\text{CN}^-$  by nucleophilic addition to the  $-\text{C}=\text{N}$  bond of the compound (Scheme 3). Test strips were prepared to evaluate the applicability of the sensor. Job's plot supported a 1:1 stoichiometry, the detection limit was  $8.6 \times 10^{-7}$  M, and the association constant ( $K$ ) was  $1.88 \times 10^4$   $\text{M}^{-1}$ . The addition mechanism was confirmed by  $^1\text{H}$  NMR experiments and FTIR spectra. The authors also used 2-formyl-1,3,5,7-tetraaryl aza-BODIPY with  $-\text{C}=\text{N}$  and  $-\text{CHO}$  functions, and it has been shown that  $\text{CN}^-$  anion prefers  $-\text{C}=\text{N}$  over  $-\text{CHO}$ .



**Scheme 3.** Proposed mechanism of the interaction **16**- $\text{CN}^-$ .

A triptycene-hydroxybenzaldehyde Schiff base **17** (Fig. 7) was proved to be a selective sensor for  $\text{CN}^-$  anion by exhibiting a turn-on in the fluorescence and a color change from orange to yellow. The mechanism includes addition of  $\text{CN}^-$  to the aldehyde moiety, and was confirmed by  $^1\text{H}$  NMR and LC-MS.<sup>45</sup>

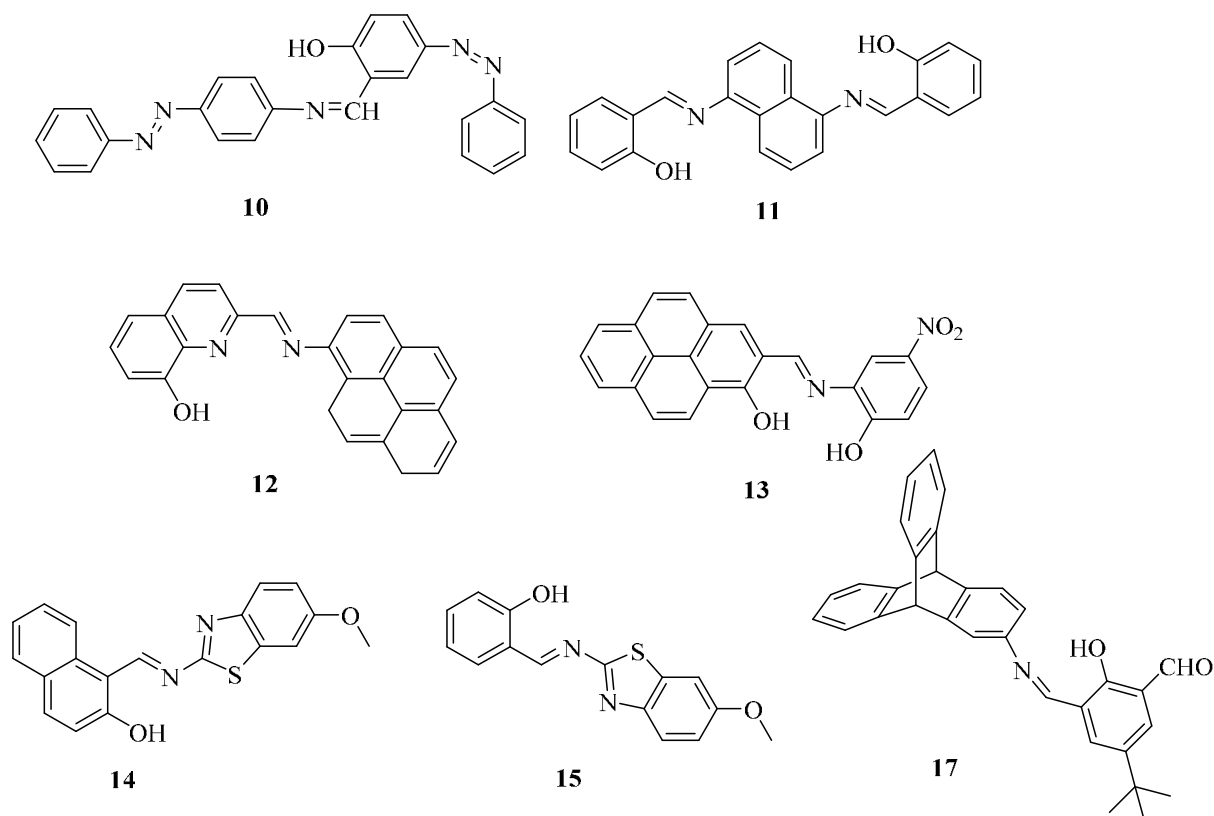
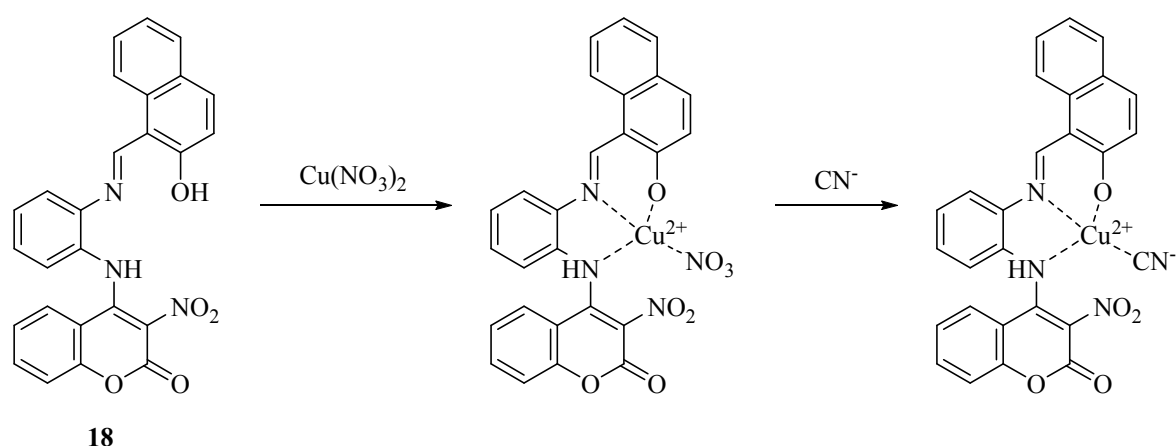


Fig. 7. Structures of chemosensors 10-15 and 17.

Schiff bases with a coumarin moiety have their own share in the sensing field. Jo et al. reported the synthesis of a new Schiff base **18** based on the combination of coumarin and naphthol groups, as a new colorimetric sensor for copper and cyanide ions.<sup>18</sup> The sensor displayed a sequential recognition of  $\text{Cu}^{2+}$  and  $\text{CN}^-$  by a colorimetric response in aqueous solution (Scheme 4).



Scheme 4. Proposed binding mode of **18**- $\text{Cu}^{2+}$  and **18**- $\text{Cu}^{2+}$ - $\text{CN}^-$  complexes.

Wang et al. developed two diethylamino coumarin Schiff bases **19**, **20** (Fig. 8) with pyridine or thiophene as terminal groups.<sup>5c</sup> The compounds act as turn-on fluorescence

chemosensors for the detection of  $\text{CN}^-$  anion. The recognition of the probes for  $\text{Cu}^{2+}$  was first investigated. The compounds responded with a color change and a quenching in the fluorescence intensity. Addition of  $\text{CN}^-$  anion led to a recovery of the color and the spectral properties of the compounds based on the copper complex ensemble displacement mechanism. The results were confirmed by DFT and TD-DFT calculations. The detection limits of compound- $\text{Cu}^{2+}$  for  $\text{CN}^-$  were  $0.019 \mu\text{M}$  and  $0.02 \mu\text{M}$  for compounds **19** and **20**, respectively.

The same group developed another “naked-eye” Schiff base chemosensor **21** (Fig. 8), this time with benzothiazole as terminal group.<sup>5d</sup> The conjugated system between coumarin and benzothiazole enables an ICT process to occur. Upon addition of  $\text{CN}^-$ , a color change is observed accompanied by a fluorescence enhancement. The mechanism is a Michael addition reaction where  $\text{CN}^-$  was added to the 4<sup>th</sup> position of the coumarin ring, thus blocking the ICT process. The same framework was investigated for the recognition of  $\text{Cu}^{2+}$ . This time the fluorescence intensity was rather quenched. The selectivity of the compound towards  $\text{CN}^-$  and  $\text{Cu}^{2+}$  was further studied by addition of other ions. A test paper experiment was also carried out. The detection limit for  $\text{CN}^-$  is  $0.007 \mu\text{M}$ .<sup>5d</sup>

Four molecules of the same series were prepared by two different groups and were tested for their sensing abilities. The Schiff bases were prepared by condensation of coumarin-thiazole hybrid molecule and a salicylaldehyde derivative. The first Schiff base **22** (Fig. 8) was prepared from *o*-vanillin by Seferoğlu's group.<sup>20</sup> It was characterized by the usual methods and using single crystal X-ray analysis. The sensing properties of **22** were first studied with different anions in DMSO using UV-vis and fluorescence spectroscopies. A bathochromic shift was observed upon addition of  $\text{F}^-$ ,  $\text{AcO}^-$  and  $\text{CN}^-$  anions due to an ICT process. The sensor showed a switch-on in the fluorescence intensity only upon addition of  $\text{CN}^-$ . The chemosensor can be restored by adding TFA. The mechanism of the interaction **22**- $\text{CN}^-$  was proposed to be a nucleophilic addition and a deprotonation of the phenolic hydrogen. It was supported by  $^1\text{H}$  NMR titrations and DFT/TD-DFT calculations. The probe also displayed a color change from yellow to deep red with  $\text{CN}^-$ , and from yellow to red upon addition of  $\text{F}^-$ ,  $\text{AcO}^-$  and  $\text{H}_2\text{PO}_4^-$ . A test was carried out in DMSO/ $\text{H}_2\text{O}$  (9:1, v/v) binary solution. A similar response was obtained with a selectivity towards  $\text{CN}^-$ , for UV-vis and fluorescence spectroscopies, and a color change from light yellow to dark yellow for  $\text{CN}^-$ , and from yellow to orange with  $\text{F}^-$  and  $\text{AcO}^-$  was observed. Pd(II) and Pt(II) complexes of the chemosensor were also prepared.<sup>20</sup>



The two next Schiff bases **23** and **24** (Fig. 8) were introduced by Sahu's group.<sup>6a</sup> The colorimetric analysis of the two compounds was tested in acetonitrile and in CH<sub>3</sub>CN/H<sub>2</sub>O (1:1, v/v) solution. In organic medium, a change from colorless to deep red and from colorless to red with **23** and **24**, respectively, was observed with F<sup>-</sup> anion, CN<sup>-</sup> and AcO<sup>-</sup> anions exhibited a faint color change and no response with the rest of the tested anions. In aqueous medium, chemosensor **23** exhibited a color change only with CN<sup>-</sup>, and **24** was not tested due to its poor solubility. UV-vis study with the anions confirmed the colorimetric results already obtained, and the changes were explained by an ICT process. A turn-on in the fluorescence intensity for compound **23** was observed with F<sup>-</sup> in CH<sub>3</sub>CN with an LOD of 0.72 μM, and with CN<sup>-</sup> in aqueous solution with an LOD of 2.7 μM. A pH study proved that the sensor could detect CN<sup>-</sup> over a range of 4-9. From <sup>1</sup>H NMR titrations, F<sup>-</sup> interacts with the probe by initial hydrogen bond formation and subsequent deprotonation, CN<sup>-</sup> interacts by hydrogen bond formation and nucleophilic addition, the results were further investigated by theoretical calculations. As an application, sensor **23** was tested in tap water.<sup>6a</sup>

Schiff base **25** (Fig. 8) was prepared once again by Seferoğlu's group.<sup>19</sup> Anion sensing ability of the compound was performed by UV-vis and fluorometric titrations. A bathochromic shift was observed upon addition of F<sup>-</sup>, AcO<sup>-</sup> and CN<sup>-</sup> to a solution of the sensor in DMSO, due to an ICT process. The anions react with a deprotonation mechanism. CN<sup>-</sup> showed an enhancement in the fluorescence intensity as a result of its addition to C=N bond. The other tested anions did not react with the receptor. The sensor displayed a color change from yellow to deep red upon addition of CN<sup>-</sup>, and from yellow to red in the case of F<sup>-</sup> and AcO<sup>-</sup>, and under UV light, only CN<sup>-</sup> showed an orange fluorescence. Geometrical optimizations and <sup>1</sup>H NMR chemical shifts were also obtained. Pt(II) and Pd(II) complexes of the Schiff base were prepared and were screened for their anti-cancer activity along with the free ligand.

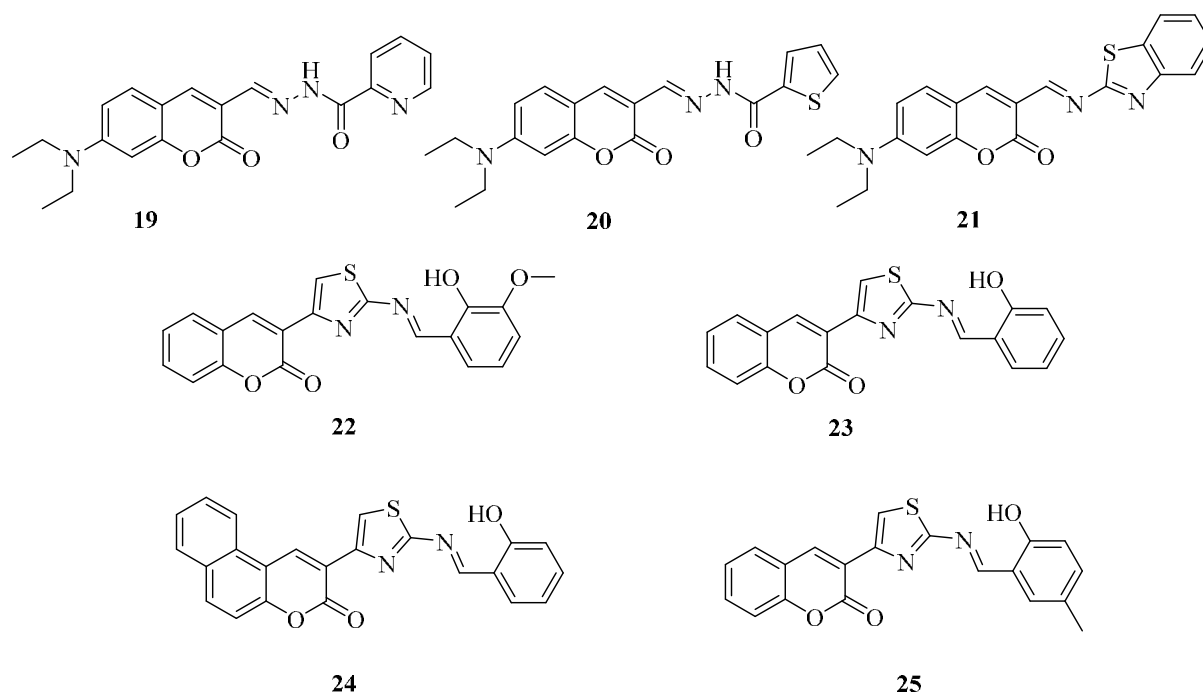


**Fig. 8.** Structures of chemosensors **19-25**.

Herein Schiff bases bearing different heterocyclic molecules and reacting as receptors for cyanide ion were described. The Schiff bases generally react with an intramolecular charge transfer (ICT) process. The presence of C=N double bond and some other groups like –OH and –NH make them susceptible to interact with cyanide anion *via* different mechanisms like deprotonation or/and addition, and alteration of hydrogen bonding. As an application, some have been investigated in the detection of CN<sup>-</sup> ion in live cells.

#### **IV. An overview on coumarin and thiophene syntheses and their biological applications**

Since their discovery by Hugo Schiff, Schiff bases play a major role in organic synthetic and medicinal chemistry. They have an azomethine group (C=N), and are typically prepared by refluxing an equimolar mixture of aldehyde or ketone and an amine in an organic medium with or without a catalyst. As mentioned before, a new series of Schiff bases was prepared from salicylaldehyde derivatives and coumarin-thiophene hybrid molecules. Coumarin (*2H*-chromen-2-one) belongs to the benzopyrones family. The coumarin skeleton can be found in many plants. Thiophene is five membered heterocyclic ring with one sulfur as the heteroatom. Thiophene and its derivatives exist in petroleum or coal.

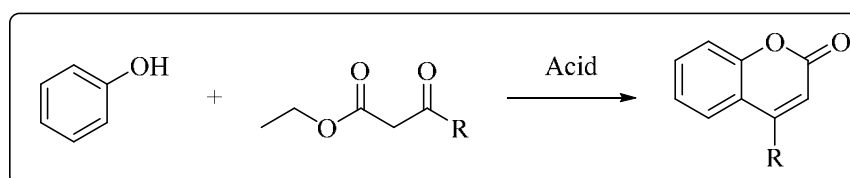
In the following, some general methods for the synthesis of coumarin and thiophene rings as well as their biological interest are described.

#### IV.1. General methods for the synthesis of coumarin

Many methods have been developed for the synthesis of the coumarin ring, including the Pechmann condensation, the Knoevenagel condensation, the Perkin reaction, the Wittig reaction and the Baylis–Hillman reaction.

##### *Pechmann condensation*

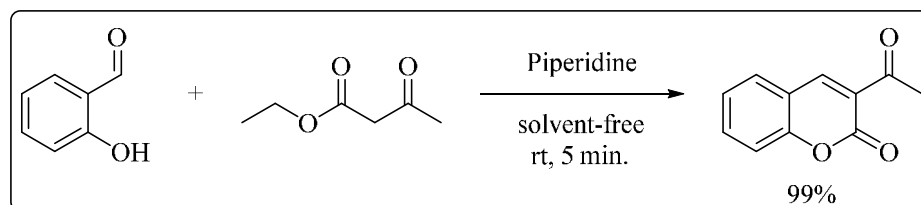
It is a reaction between a phenol and a  $\beta$ -keto ester or a  $\beta$ -keto carboxylic acid with an acid catalyst (Scheme 5). The Pechmann condensation is one of the widely used methods in the preparation of coumarin derivatives due to its simplicity and the availability of the starting materials. It was first reported by Pechmann and Duisberg in 1883. Many procedures have been adapted to the Pechman method such as reactions under MW irradiations<sup>46,47</sup> and the use of catalysts in a solvent-free system.<sup>48</sup>



**Scheme 5.** Synthesis of coumarin *via* Pechmann condensation

##### *Knoevenagel condensation*

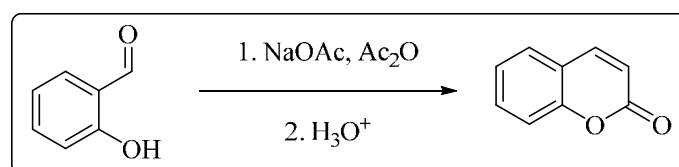
Knoevenagel condensation is one of the most important methods of the synthesis of 3-substituted coumarins. It involves the condensation of a salicylaldehyde derivative with activated methylene compounds like diethyl malonate, ethylcyanoacetate and ethyl acetoacetate in the presence of an amine as catalyst with or without ethanol as solvent.<sup>49</sup> 3-acetyl coumarin was prepared by Knoevenagel reaction in solvent-free condition with piperidine as a catalyst in 5 minutes at room temperature (Scheme 6).<sup>50</sup>



**Scheme 6.** Synthesis of 3-acetyl coumarin *via* Knoevenagel condensation

*Perkin reaction*

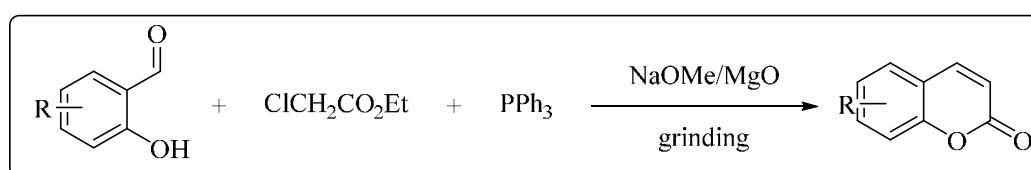
The Perkin reaction is originally used in the synthesis of cinnamic acid derivatives by the thermal condensation between an aromatic aldehyde and acid anhydrides or carboxylic derivatives in the presence of a base catalyst.<sup>51</sup> When salicylaldehydes are used, coumarins are obtained (Scheme 7).



**Scheme 7.** Perkin coumarin synthesis

*Synthesis of coumarins by Wittig reaction*

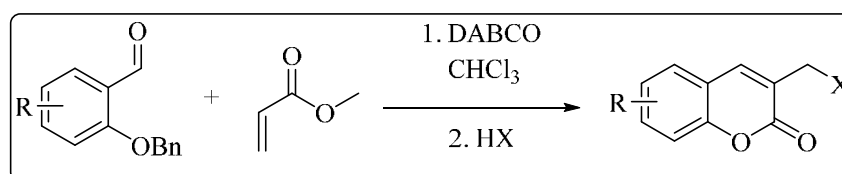
Wittig reaction approach involves the reaction of an aromatic aldehyde with a phosphonate or phosphorous ylide. Shockravi et al<sup>52</sup> reported a Wittig reaction of an *in situ* prepared carbethoxymethylenetriphenylphosphorane and salicylaldehydes supported on MgO for a rapid synthesis of simple coumarins in solvent-free condition (Scheme 8).



**Scheme 8.** Synthesis of coumarin by Wittig reaction

*Baylis–Hillman reaction*

Coumarins were synthesized by the Baylis-Hillman reaction by reacting salicylaldehyde with *t*-butyl acrylate in the presence of DABCO as a catalyst.<sup>53</sup> The Baylis-Hillman adducts formed were then reacted with HI or HCl in acetic acid to form 3-(iodomethyl)coumarin or 3-(chloromethyl)coumarin derivatives (Scheme 9).



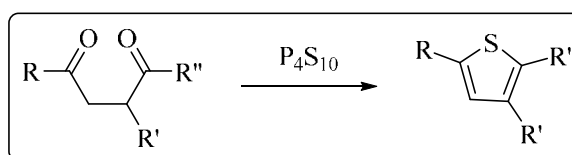
**Scheme 9.** Synthesis of coumarin by Baylis–Hillman reaction

## IV.2. Synthetic routes for thiophene nucleus formation

Herein the major synthetic procedures for thiophene formation are described, this includes: Paal-Knorr thiophene synthesis, Fiesselmann thiophene synthesis, Gewald aminothiophene synthesis and Hinsberg synthesis.

### *Paal-Knorr thiophene synthesis*

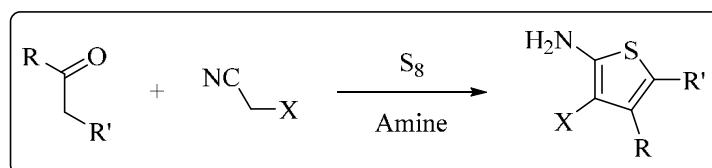
The Paal-Knorr thiophene synthesis is the condensation of a 1,4-dicarbonyl compound in the presence of an excess of a source of sulfur such as phosphorous pentasulfide (Scheme 10).<sup>54</sup>



**Scheme 10.** The Paal-Knorr thiophene synthesis

### *Gewald synthesis*

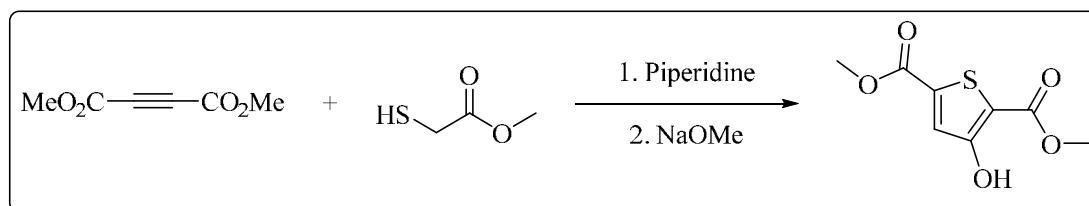
The first version of Gewald aminothiophene synthesis consists of a reaction between an  $\alpha$ -thio carbonyl compound and an activated nitrile in the presence of a basic catalyst (usually triethylamine or piperidine). The second version is a multicomponent condensation of sulfur, an  $\alpha$ -methylene carbonyl and an activated nitrile such as malononitrile or cyanoacetic esters in the presence of an amine as catalyst (Scheme 11).<sup>55</sup> The last version is a two-step procedure where sulfur is treated with an  $\alpha,\beta$ -unsaturated nitrile first regenerated by a Knoevenagel-Cope condensation.<sup>56</sup> A variety of substituted 2-aminothiophenes can be synthesized using those three variants.



**Scheme 11.** The second version of Gewald synthesis of thiophene

### *Fiesselmann thiophene synthesis*

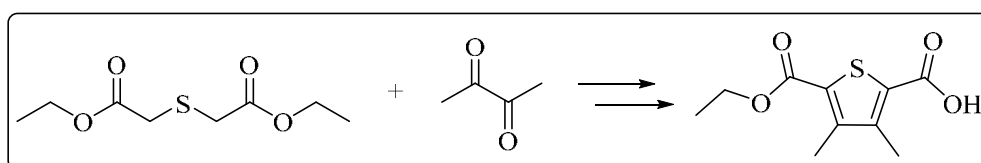
It is the condensation reaction of thioglycolic acid with  $\alpha$ ,  $\beta$ -acetylenic esters leading to the formation of 3- hydroxyl- 2- thiophenecarboxylic acid derivatives, by treatment with a base<sup>54</sup> (Scheme 12).



**Scheme 12.** Fiesselmann thiophene synthesis

### *Hinsberg synthesis*

The Hinsberg thiophene synthesis was reported in 1910 by the German chemist Oscar Hinsberg. In this reaction, diketones are reacted with thioglutaric diesters in the presence of a base leading to substituted thiophenes.<sup>57</sup> Scheme 13 shows the reaction using diacetyl, a strong non-nucleophilic base like potassium tert-butoxide can be used.



**Scheme 13.** Hinsberg synthesis of thiophene

Knoevenagel coumarin synthesis along with Gewald aminothiophene condensation were part of the procedures used in order to prepare our target molecules.

### **IV.3. Medicinal applications of coumarin and thiophene derivatives**

Besides their vast use in the sensing field, coumarins are known for having many biological activities, for instance antioxidant,<sup>58</sup> anticoagulant,<sup>59</sup> antibacterial,<sup>60</sup> antifungal<sup>61</sup> and anticancer.<sup>62</sup> Coumarin represents the core structure of several natural and synthetic molecules with pharmaceutical importance, such as umbelliferone reported having antioxidant properties, novobiocin which is an antibiotic, warfarin, acenocoumarol and dicoumarol are anticoagulant agents. Some examples of biologically active coumarin derivatives are shown in Fig. 9.

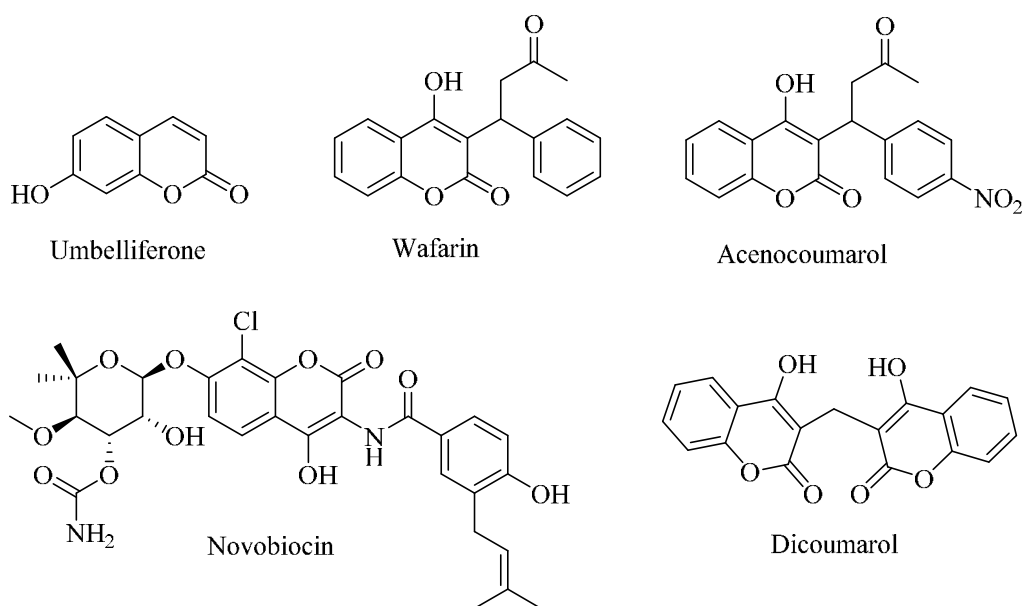


**Fig. 9.** Biologically active coumarin derivatives.

Thiophene is also known for having diverse activities.<sup>54</sup> It is used either as central ring or as a part of a fused ring system. Some commercialized drugs containing thiophene moiety are: Arotinolol and Eprosartan used in the treatment of high blood pressure, Articaine used as a dental local anesthetic, Azosemide is a high-ceiling diuretic agent, Suprofen is a non-steroidal anti-inflammatory drug and Duloxetine which is prescribed for major depressive disorder and generalized anxiety disorder (Fig. 10).<sup>63</sup>

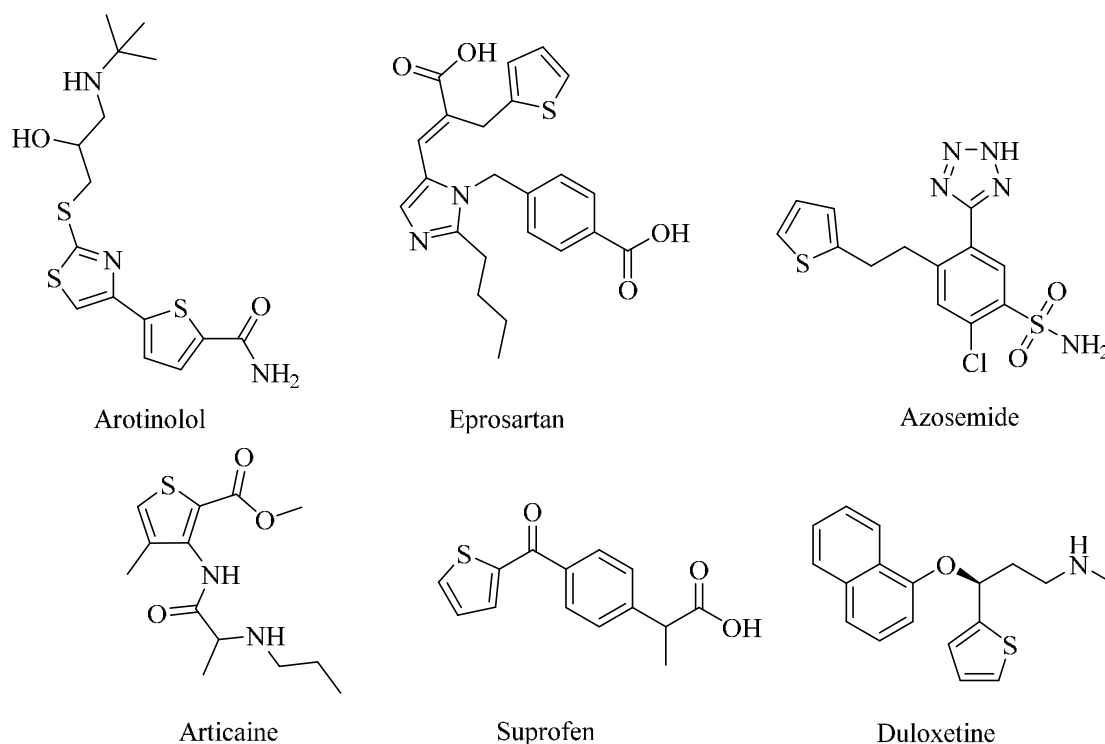


**Fig. 10.** Biologically active thiophene derivatives.

Among the methods used for developing novel bioactive compounds is “molecular hybridization”. It was shown that the association of another heterocyclic compound with coumarin, as a substituent or a fused component, changes its properties and generally improves the activity.<sup>64</sup> Thus a combination of coumarin and thiophene moieties besides the presence of an azomethine group may give more active molecules.



## References

- [1] Xu, Z.C.; Chen, X. Q.; Kim, H. N.; Yoon, J. Y. *Chem. Soc. Rev.* **2010**, 39, 127-137.
- [2] (a) Babür, B.; Seferoğlu, N.; Seferoğlu, Z. *Tetrahedron Lett.* **2015**, 56, 2149-2154. (b) Pangannaya, S.; Mohan, M.; Trivedi, D. R. *New J. Chem.* **2018**, 42, 10406-10413.
- [3] Valeur, B. “*Molecular Fluorescence Principles and Applications*” Wiley-VCH Verlag GmbH, New York, **2001**.
- [4] (a) Murtaza, G.; Mumtaz, A.; Khan, F. A.; Ahmed, S.; Azhar, S.; Najam-Ul-Haq, M.; Atif, M.; Khan, S. A.; Maalik, A.; Alam, F.; Hussain, I. *Acta Pol. Pharm.* **2014**, 71, 531-535. (b) Qin, W.; Long, S.; Panunzio, M.; Biondi, S. *Molecules* **2013**, 18, 12264-12289.
- [5] (a) Wu, J. S.; Liu, W. M.; Zhuang, X. Q.; Wang, F.; Wang, P. F.; Tao, S. L.; Zhang, X. H.; Wu, S. K.; Lee, S. T. *Org. Lett.* **2007**, 9, 33-36. (b) Lin, W.; Yuan, L.; Cao, X. *Tetrahedron Lett.* **2008**, 49, 6585-6588. (c) Wang, K.; Ma, L.; Liu, G.; Cao, D.; Guan, R.; Liu, Z. *Dyes and Pigments* **2016**, 126, 104-109. (d) Wang, K.; Feng, W.; Wang, Y.; Cao, D.; Guan, R.; Yu, X.; Wu, Q. *Inorg. Chem. Commun.* **2016**, 71, 102-104. (e) Wani, M. A.; Singh, P. K.; Pandey, R.; Pandey, M. D. *J. Lumin.* **2016**, 171, 159-165. (f) Yang, M.; Wang, H.; Huang, J.; Fang, M.; Mei, B.; Zhou, H.; Wu, J.; Tian, Y. *Sens. Actuators, B* **2014**, 204, 710-715. (g) Yeh, J. T.; Chen, W. C.; Liu, S. R.; Wu, S. P. *New J. Chem.* **2014**, 38, 4434-4439. (h) Li, Z.; Zhou, Y.; Yin, K.; Yu, Z.; Li, Y.; Ren, J. *Dyes and Pigments* **2014**, 105, 7-11. (i) Wang, L.; Ye, D.; Cao, D. *Spectrochim. Acta, Part A* **2012**, 90, 40-44.
- [6] (a) Padhan, S. K.; Podh, M. B.; Sahu, P. K.; Sahu, S. N. *Sens. Actuators, B* **2018**, 255, 1376-1390. (b) Wan, L.; Shu, Q.; Zhu, J.; Jin, S.; Li, N.; Chen, X.; Chen, S. *Talanta* **2016**, 152, 39-44. (c) Zhang, P.; Shi, B. B.; You, X. M.; Zhang, Y. M.; Lin, Q.; Yao, H.; Wei, T. B. *Tetrahedron* **2014**, 70, 1889-1894. (d) Barare, B.; Yıldız, M.; Alpaslan, G.; Dilek, N.; Unver, H.; Tadesse, S.; Aslan, K. *Sens. Actuators, B* **2015**, 215, 52-61.
- [7] Fayed, T.; EL-Morsi, M.; EL-Nahass, M. *J. Chem. Sci.* **2013**, 125, 883-894.
- [8] Gore, M. G. “*Spectrophotometry and Spectrofluorimetry A Practical Approach*” Oxford University Press, USA, **2000**.
- [9] Glossary of terms used in photochemistry, 3rd edition (IUPAC Recommendations 2006).

- [10] Wang, B.; Anslyn, E. V. “*Chemosensors Principles, Strategies, and Applications*” Wiley Series in Drug Discovery and Development, **2011**.
- [11] Gale, P. A.; Caltagirone, C. *Coord. Chem. Rev.* **2018**, 354, 2-27.
- [12] Wu, J.; Liu, W.; Ge, J.; Zhang, H.; Wang, P. *Chem. Soc. Rev.* **2011**, 40, 3483-3495.
- [13] Yanar, U. ; Babür, B. ; Pekyılmaz, D. ; Yahaya, I. ; Aydın, B. ; Dede, Y. ; Seferoğlu, Z. *J. Mol. Struct.* **2016**, 1108, 269-277.
- [14] Zhou, X.; Lv, X.; Hao, J.; Liu, D.; Guo, W. *Dyes and Pigments* **2012**, 95, 168-173.
- [15] Cheng, X.; Tang, R.; Jia, H.; Feng, J.; Qin, J.; Li, Z. *Appl. Mater. Interfaces* **2012**, 4, 4387-4392.
- [16] Kim, H. J.; Ko, K. C.; Lee, J. H.; Lee, J. Y.; Kim, J. S. *Chem. Commun.* **2011**, 47, 2886-2888.
- [17] Shiraishi, Y.; Nakamura, M.; Matsushita, N.; Hirai, T. *New J. Chem.* **2016**, 40, 195-201.
- [18] Jo, H. Y.; Park, G. J.; Na, Y. J.; Choi, Y. W.; You, G. R.; Kim, C. *Dyes and Pigments* **2014**, 109, 127-134.
- [19] Şahin, Ö.; Özdemir, Ü. Ö.; Seferoğlu, N.; Genc, Z. K.; Kaya, K.; Aydın, B.; Tekin, S.; Seferoğlu, Z. *J. Photochem. Photobiol., B* **2018**, 178, 428-439.
- [20] Şahin, Ö.; Özdemir, Ü. Ö.; Seferoğlu, N.; Aydın, B.; Sarı, M.; Tunç, T.; Seferoğlu, Z. *Tetrahedron* **2016**, 72, 5843-5852.
- [21] Wang, L.; Li, L.; Cao, D. *Sensors and Actuators B: Chemical* **2017**, 241, 1224-1234.
- [22] Dvivedi, A.; Kumar, S.; Ravikanth, M. *Sens. Actuators, B* **2016**, 224, 364-371.
- [23] Liu, Y. W.; Kao, M. X.; Wu, A. T. *Sens. Actuators, B* **2015**, 208, 429-435.
- [24] Zhou, X.; Kim, J.; Liu, Z.; Jo, S.; Pak, Y. L.; Swamy, K. M. K.; Yoon, J. *Dyes and Pigments* **2016**, 128, 256-262.
- [25] Manivannan, R.; Satheskumar, A.; El-Mossalamy, E. H.; Al-Harbi, L. M.; Kosa, S. A.; Elango, K. P. *New J. Chem.* **2015**, 39, 3936-3947.

- [26] Hu, F.; Cao, M.; Huang, J.; Chen, Z.; Wu, D.; Xu, Z.; Liu, S. H.; Yin, J. *Dyes and Pigments* **2015**, 119, 108-115.
- [27] Suganya, S.; Velmathi, S. *Sens. Actuators, B* **2015**, 221, 1104-1113.
- [28] Yang, L.; Li, X.; Yang, J.; Qu, Y.; Hua, J. *Appl. Mater. Interfaces* **2013**, 5, 1317-1326.
- [29] Wang, S. T.; Sie, Y. W.; Wan, C. F.; Wu, A. T. *J. Lumin.* **2016**, 173, 25-29.
- [30] Mahapatra, A. K.; Mondal, S.; Manna, S. K.; Maiti, K.; Maji, R.; Uddin, Md. R.; Mandal, S.; Sarkar, D.; Mondal, T. K.; Maitid, D. K. *Dalton Trans.* **2015**, 44, 6490-6501.
- [31] Wani, M. A.; Singh, P. K.; Pandey, R.; Pandey, M. D. *J. Lumin.* **2016**, 171, 159-165.
- [32] Yeh, J. T.; Chen, W. C.; Liu, S. R.; Wu, S. P. *New J. Chem.* **2014**, 38, 4434-4439.
- [33] You, G. R.; Lee, J. J.; Choi, Y. W.; Lee, S. Y.; Kim, C. *Tetrahedron* **2016**, 72, 875-881.
- [34] Gupta, N.; Singhal, D.; Singh, A. K. *New J. Chem.* **2016**, 40, 641-650.
- [35] Wang, S. T.; Chir, J. L.; Jhong, Y.; Wu, A. T. *J. Lumin.* **2015**, 167, 413-417.
- [36] Singh, Y.; Ahmad, I.; Ghosh, T. *Sens. Actuators, B* **2017**, 242, 1079-1085.
- [37] Li, Q.; Zhang, J.; Cai, Y.; Qu, W.; Gao, G.; Lin, Q.; Yao, H.; Zhang, Y.; Wei, T. *Tetrahedron* **2015**, 71, 857-862.
- [38] Zhu, X.; Lin, Q.; Lou, J. C.; Lu, T. T.; Zhang, Y. M.; Wei, T. B. *New J. Chem.* **2015**, 39, 7206-7210.
- [39] Hu, J. H.; Li, J. B.; Qi, J.; Sun, Y. *New J. Chem.* **2015**, 39, 4041-4046.
- [40] Lee, J. J.; Park, G. J.; Choi, Y. W.; You, G. R.; Kim, Y. S.; Lee, S. Y.; Kim, C. *Sens. Actuators, B* **2015**, 207, 123-132.
- [41] Lee, H. J.; Park, S. J.; Sin, H. J.; Na, Y. J.; Kim, C. *New J. Chem.* **2015**, 39, 3900-3907.
- [42] Udhayakumari, D.; Velmathi, S.; Boobalan, M. S. *J. Fluorine Chem.* **2015**, 175, 180-184.
- [43] Zhang, X.; Chen, S.; Jin, S.; Zhang, Y.; Chen, X.; Zhang, Z.; Shu, Q. *Sens. Actuators, B* **2017**, 242, 994-998.

- [44] Barare, B.; Yıldız, M.; Ünver, H.; Aslan, K. *Tetrahedron Lett.* **2016**, 57, 537-542.
- [45] Emandi, G.; Browne, M. P.; Lyons, M. E.; Prior, C.; Senge, M. O. *Tetrahedron* **2017**, 73, 2956-2965.
- [46] Manhas, M. S.; Ganguly, S. N.; Mukherjee, S.; Jain, A. K.; Bose, A. K. *Tetrahedron Lett.* **2006**, 47, 2423-2425.
- [47] Valizadeh, H.; Kordi, F. M.; Gholipur, H.; Amiri, M. *Phosphorus Sulfur Silicon Relat. Elem.* **2009**, 184, 3075-3081.
- [48] Suprita, S.; Singh, R. *Int. J. Chem. Stud.* **2017**, 5, 707-711.
- [49] Vekariya, R. H.; Patel, H. D. *Synth. Commun.* **2014**, 44, 2756-2788.
- [50] Sugino, T.; Tanaka, K. *Chem. Lett.* **2001**, 30, 110.
- [51] Perkin, W. H. *J. Chem. Soc.* **1868**, 21, 53.
- [52] Shockravi, A.; Valizadeh, H.; Heravi, M. M. *Phosphorus Sulfur Silicon Relat. Elem.* **2003**, 178, 501-504.
- [53] Kaye, P.T.; Musa, M. A. *Synthesis* **2002**, 18, 2701-2706.
- [54] Mishra, R.; Jha, K.K.; Kumar, S.; Tomer, I. *Der Pharma Chem.* **2011**, 3, 38-54.
- [55] Puterová, Z.; Krutošiková, A.; Végh, D. *ARKIVOC* **2010** (i) 209-246.
- [56] Sabnis, R. W. *Sulfur Reports* **1994**, 16, 1-17.
- [57] Wynberg, H.; Kooreman, H. J. *J. Am. Chem. Soc.* **1965**, 87, 1739-1742.
- [58] Kadhum, A. A. H.; Al-Amiery, A. A.; Musa, A. Y.; Mohamad, A. B. *Int. J. Mol. Sci.* **2011**, 12, 5747-5761.
- [59] Weigt, S.; Huebler, N.; Strecker, R.; Braunbeck, T.; Broschard, T. H. *Reprod. Toxicol.* **2012**, 33, 133-141.
- [60] de Souza, S. M.; Delle Monache, F.; Smania, A. Z. *Naturforsch. C* 2005, 60, 693-700.
- [61] Sardari, S.; Mori, Y.; Horita, K.; Micetich, R. G.; Nishibe, S.; Daneshtalab, M. *Bioorgan. Med. Chem.* **1999**, 7, 1933-1940.

[62] Thakur, A.; Singla, R.; Jaitak, V. *Eur. J. Med. Chem.* **2015**, 101, 476-495.

[63] (a) Zhao, J.; Golozoubova, V.; Cannon, B.; Nedergaard, J. *Can. J. Physiol. Pharmacol.* **2001**, 79, 585-593. (b) Oertel, R.; Ebert, U.; Rahn, R.; Kirch, W. *Clin. Pharmacokinet.* **1997**, 33, 417-425. (c) Higley, C. A.; Wilde, R. G.; Maduskuie, T. P.; Johnson, A. L.; Pennev, P.; Billheimer, J. T.; Robinson, C. S.; Gillies, P. J.; Wexler, R. R. *J. Med. Chem.* **1994**, 37, 3511-3522. (d) Bymaster, F. P.; Beedle, E. E.; Findlay, J. *Bioorg. Med. Chem. Lett.* **2003**, 13, 4477-4480.

[64] (a) Silva, F. T.; Franco, C. H.; Favaro, D. C.; Freitas, L. H.; Moraes, C. B.; Ferreira, E. I. *Eur. J. Med. Chem.* **2016**, 121, 553-560. (b) Kahveci, B.; Yılmaz, F.; Menteşe, E.; Ulker, S. *Arch. Pharm. Chem. Life Sci.* (2017) 350, e1600369.

MCours.com